

Figure 2. ORTEP drawing of **3** showing the anionic moiety with the labeling scheme. Thermal ellipsoids are drawn at the 50% probability level. Selected values of bond distances (Å) and angles (deg) are as follows: Ti(1)–N(1) = 2.066 (13), Ti(1)–N(3) = 2.236 (19), Ti(1)–N(4) = 2.290 (13), N(1)–Si(1) = 1.726 (14), Ti(1)–Ti(1a) = 3.680 (8), N(3)–N(4) = 1.379 (21), N(1)–Ti(1)–Ni(1a) = 107.0 (5), Ti(1)–N(1)–Si(1) = 123.0 (8).

The chemical connectivity of **3** was also demonstrated by X-ray diffraction analysis. The structure consists of two separate $[\text{Li}(\text{TMEDA})_2]$ and $[\{(\text{Me}_3\text{Si})_2\text{N}\}_2\text{Ti}\}_2(\mu\text{-}\eta^2\text{-}\eta^2\text{-N}_2)_2]$ ionic fragments. The Ti-containing unit is dinuclear and is formed by two $[(\text{Me}_3\text{Si})_2\text{N}]_2\text{Ti}$ groups symmetrically and perpendicularly placed on the two sides of the plane defined by two parallel molecules of dinitrogen (Figure 2). Four of the six coordination sites of titanium are occupied by the four nitrogen atoms of the two coplanar dinitrogen molecules, the two remaining sites being occupied by the two amido groups. The side-on geometry of the two coordinated N_2 molecules is somewhat reminiscent of that of a recently reported zirconium dinitrogen phosphine complex.¹² Even in this case, the N–N distance [N(3)–N(4) = 1.379 (21) Å] is rather long, and it is significantly longer than that displayed by complex **1**. By contrast, the Ti–N distances [Ti(1)–N(3) = 2.236 (19) Å, Ti(1)–N(4) = 2.290 (13) Å] are definitely longer as a probable result of the different fashion of bonding. It is quite difficult to speculate on the extent of dinitrogen reduction on the exclusive basis of the N–N distances, since the structural features of **3** (with no particularly long N–N and Ti–N distances) are somehow in contradiction with those of **1** (with comparable N–N distance and extremely short Ti–N distance). The completely different bonding mode of dinitrogen in the two complexes (end-on versus side-on) is intriguing indeed and at the moment can be explained only by the different steric bulk of the two complexes.

As expected, complex **1** is diamagnetic while **2** and **3** are paramagnetic [μ_{eff} = 1.75 μ_{B} , μ_{eff} = 1.37 μ_{B} , respectively]. The low value of the magnetic moment of **3** can be ascribed to either antiferromagnetic or superexchange, since the Ti...Ti nonbonding distance is rather short [Ti(1)–Ti(1a) = 3.680 (8) Å].

Acknowledgment. This work was supported by the Natural Sciences and Engineering Research Council of Canada (operating grant) and the Petroleum Research Funds administered by the American Chemical Society.

Supplementary Material Available: Tables listing atomic positional parameters, anisotropic thermal parameters, and complete bond distances and angles for **1** and **3**, and an ORTEP plot for $\text{Li}(\text{TMEDA})_2$ (15 pages); tables of observed and calculated structure factors for **1** and **3** (21 pages). Ordering information is given on any current masthead page.

Photoluminescence of Antimony(III) and Bismuth(III) Chloride Complexes in Solution

Hans Nikol and Arnd Vogler*

Institut für Anorganische Chemie
Universität Regensburg, Universitätsstrasse 31
D-8400 Regensburg, Federal Republic of Germany

Received May 28, 1991

Revised Manuscript Received September 17, 1991

Metal-centered (MC) excited states play an important role in the photophysics and photochemistry of coordination compounds.¹ However, the study of MC states has been essentially limited to d and f block elements, while the main group metals were largely ignored.² This lack of knowledge is quite surprising since MC excited states of many main group metal complexes can be easily studied by emission spectroscopy under ambient conditions. Although simple halide complexes of s^2 metals such as Ti^+ , Sn^{2+} , Pb^{2+} , and Sb^{3+} are known to be luminescent in solution,² this observation has been occasionally used only for analytical applications but hardly for the characterization of the emitting excited state. On the contrary, the emission of s^2 ions which are doped into host lattices has been studied in detail by solid-state physicists.^{3,4} We report here our observations on the photoluminescence of SbCl_4^- , SbCl_6^{3-} , BiCl_4^- , and BiCl_6^{3-} in solution and discuss the nature of the emitting excited state. While an emission of SbCl_6^{3-} in CHCl_3 has been reported before,^{5,6} the other three complex ions are not yet known to show photoluminescence in solution at room temperature.

The compounds $[\text{NET}_4]\text{SbCl}_4$ and $[\text{NET}_4]\text{BiCl}_4$ were prepared according to a published procedure.⁷ The complex ions SbCl_6^{3-} and BiCl_6^{3-} in acetonitrile were formed by the addition of an excess of $[\text{NET}_4]\text{Cl}$ to the MCl_4^- ions. The absorption spectrum of SbCl_4^- in acetonitrile (Figure 1) displays three bands (Table I). Light absorption by SbCl_4^- was accompanied by a red emission (Figure 1, Table I). The excitation spectrum agreed well with the absorption spectrum. Upon addition of chloride SbCl_4^- was converted to SbCl_6^{3-} which has an absorption spectrum (Figure 1, Table I) similar to that of SbCl_4^- . Light absorption by SbCl_6^{3-} led to a green emission (Figure 1, Table I). Again, the excitation spectrum matched the absorption spectrum. If light absorption was complete ($A > 2$), the progressive conversion of SbCl_4^- to SbCl_6^{3-} was accompanied by the appearance of an isoemissive point at $\lambda = 613$ nm. The absorption and emission spectra of BiCl_4^- and BiCl_6^{3-} (Figure 2) showed features (Table I) which are analogous to those of SbCl_4^- and SbCl_6^{3-} . In contrast to the antimony complexes, the B band of the bismuth compounds was not observed in accordance with results on $\text{Cs}_2\text{NaYCl}_6$ doped with Bi^{3+} .⁸

According to the VSEPR model⁹ the structures of complexes of s^2 metal ions should be determined by the presence of a stereochemically active lone pair. However, s^2 complexes with a coordination number of six are generally octahedral, and thus they are exceptions from the rule.^{10,11} This applies also to the structures

(1) (a) Balzani, V.; Carassiti, V. *Photochemistry of Coordination Compounds*; Academic Press: New York, 1970. (b) *Concepts of Inorganic Photochemistry*; Adamson, A. W., Fleischauer, P. D., Eds.; Wiley-Interscience: New York, 1975. (c) Ferraudi, G. J. *Elements of Inorganic Photochemistry*; Wiley-Interscience: New York, 1988.

(2) Vogler, A.; Paukner, A.; Kunkely, H. *Coord. Chem. Rev.* **1990**, *97*, 285.

(3) (a) Blasse, G. *Prog. Solid St. Chem.* **1988**, *18*, 79. (b) Blasse, G. *Rev. Inorg. Chem.* **1983**, *5*, 319.

(4) Ranfagni, A.; Mugnai, D.; Bacci, M.; Viliiani, G.; Fontana, M. P. *Adv. Phys.* **1983**, *32*, 823.

(5) Vogler, A.; Paukner, A. *Inorg. Chim. Acta* **1989**, *163*, 207.

(6) Blasse, G.; Vogler, A. *Inorg. Chim. Acta* **1990**, *170*, 149.

(7) Ahliah, G. Y.; Goldstein, M. J. *Chem. Soc. (A)* **1970**, 326.

(8) Van der Steen, A. C. *Phys. Stat. Sol. (B)* **1980**, *100*, 603.

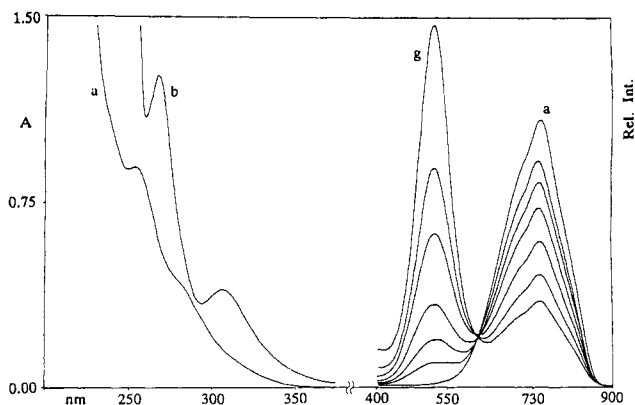
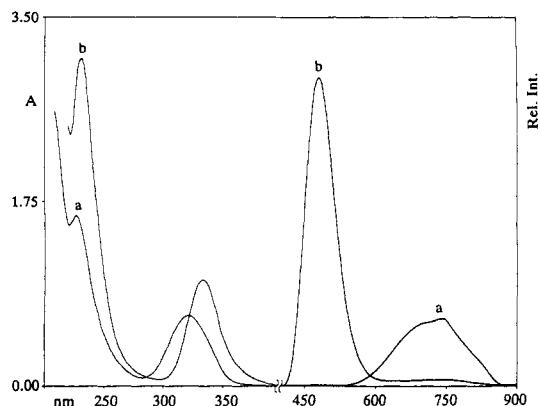
(9) (a) Gillespie, R. J.; Nyholm, R. S. *Q. Rev. Chem. Soc.* **1957**, *11*, 339. (b) Gillespie, R. J. *Molecular Geometry*; Van Nostrand Reinhold: London, 1972.

(10) Du Bois, A.; Abriel, W. Z. *Naturforsch.* **1990**, *45B*, 573 and references therein.

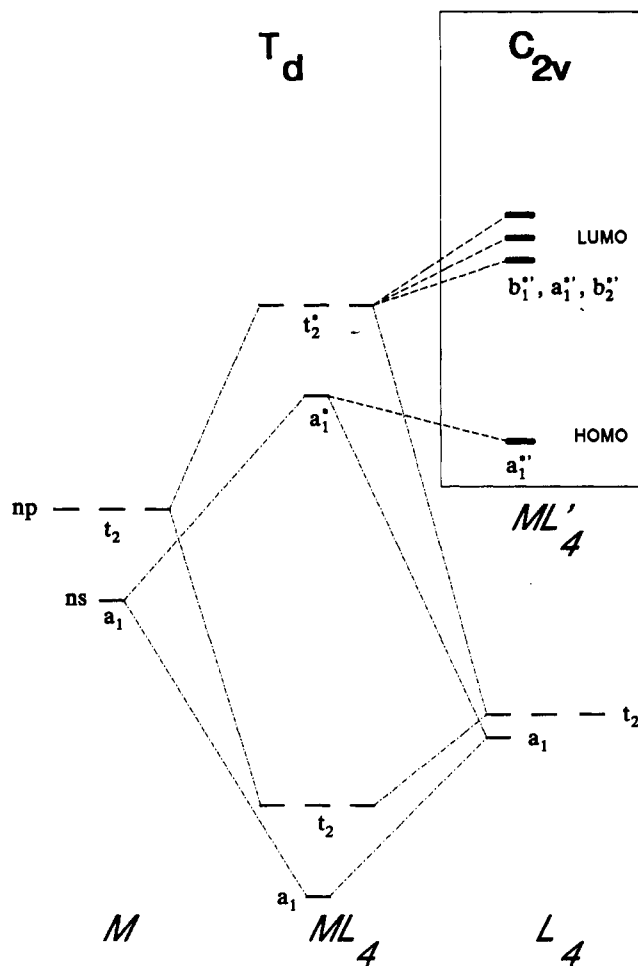
(12) Fryzuk, M. D.; Haddad, T. S.; Rettig, S. J. *J. Am. Chem. Soc.* **1990**, *112*, 8185.

Table I. Absorption and Emission Spectra of MCl_4^- and MCl_6^{3-} ($\text{M} = \text{Sb, Bi}$) in CH_3CN at Room Temperature

	SbCl_4^-	SbCl_6^{3-}	BiCl_4^-	BiCl_6^{3-}
absorption, λ_{max} [nm]				
(ϵ [$1 \text{ mol}^{-1} \text{ cm}^{-1}$])				
A band	283	306	319	333
	(1600)	(1600)	(5100)	(10300)
B band	255	267		
	(3500)	(5000)		
C band	235	242	227	231
	(5000)	(13300)	(12300)	(36000)
emission, λ_{max} [nm]	740	520	720	475
ϕ ($\times 10^3$)	6.1	1.3	10.0	4.0
stokes shift [cm^{-1}]	21800	13500	17500	9000

**Figure 1.** Electronic absorption (left side) and emission (right side) spectra of $[\text{NET}_4]\text{SbCl}_4$ in acetonitrile at room temperature, 1-cm cell. Absorption: $2.54 \times 10^{-4} \text{ M}$ (a) and in the presence of 0.1 M $[\text{NET}_4]\text{Cl}$ (b). Emission: $5.0 \times 10^{-4} \text{ M}$ (a) and in the presence of 0.008, 0.01, 0.02, 0.04, 0.06, and 0.08 M $[\text{NET}_4]\text{Cl}$ (g) $\lambda_{\text{exc}} = 290 \text{ nm}$, intensity in arbitrary units.**Figure 2.** Electronic absorption (left side) and emission (right side) spectra of $[\text{NET}_4]\text{BiCl}_4$ in acetonitrile at room temperature, 1-cm cell. Absorption: $1.08 \times 10^{-4} \text{ M}$ (a) and in the presence of 0.05 M $[\text{NET}_4]\text{Cl}$ (b). Emission: $4.0 \times 10^{-4} \text{ M}$ (a) and in the presence of 0.033 M $[\text{NET}_4]\text{Cl}$ (b), $\lambda_{\text{exc}} = 313 \text{ nm}$, intensity in arbitrary units.

of SbCl_6^{3-} ^{5,12,13} and BiCl_6^{3-} ^{12,14} which are octahedral. The absorption spectra of both complexes are characterized by MC $s \rightarrow p$ transitions from the HOMO a^*_{1g} to the LUMO t^*_{1u} . This transition gives rise to three absorption bands (Table I) which originate from the transitions of the free s^2 ions: $^1S_0 \rightarrow ^3P_1$ (A

**Figure 3.** Qualitative MO scheme of MCl_4^- ($\text{M} = \text{Sb, Bi}$) in T_d and C_{2v} (butterfly structure) symmetry; π orbitals of the ligands are omitted.

band), 3P_2 (B), 1P_1 (C)³⁻⁶ or in O_h symmetry $^1A_{1g} \rightarrow ^3T_{1u}$, $^3T_{1u}$, $^1T_{1u}$.⁵ The emission is then assigned to the $^3P_1 \rightarrow ^1S_0$ (or $^3T_{1u} \rightarrow ^1A_{1g}$) transition. A Stokes shift of this magnitude (Figure 1 and 2; Table I) has been observed before.^{5,6}

The structures of s^2 complexes with coordination numbers smaller than six are generally in agreement with the VSEPR model and deviate from the highest possible symmetry due to the presence of the stereochemically active lone pair.¹⁵ The ions SbCl_4^- and BiCl_4^- are thus not tetrahedral but distorted most likely to a butterfly structure (C_{2v} symmetry).^{7,17,18} In terms of a qualitative MO scheme (Figure 3) this distortion is caused by a stabilization (second-order Jahn-Teller effect) of the HOMO which is achieved by $sp(a'_1)$ orbital mixing.²⁰ The $s \rightarrow p$ transition ($a_1 \rightarrow t_2^*$ in T_d or $a'_1 \rightarrow b'_1, a'_1, b'_2$ in C_{2v} symmetry) splits again into the three components $^1S_0 \rightarrow ^3P_1$ (A band), 3P_2 (B), and 1P_1 (C) of the free M^{3+} ions. The absorption spectra of MCl_4^- are thus rather similar to those of MCl_6^{3-} (Figure 1 and 2; Table I). On the contrary, the emissions of MCl_4^- appear at much larger wavelength than those of MCl_6^{3-} . The huge Stokes shift of MCl_4^- (Table I) is indicative of a very large structural change associated with the electronic excitation.

(15) In the solid-state polymeric structures which are associated with an expansion of the coordination number are frequently formed.^{13,16}

(16) Blazic, B.; Lazarini, F. *Acta Crystallogr.* **1985**, *C41*, 1619.

(17) Work, R. A.; Good, M. L. *Spectrochim. Acta* **1973**, *29A*, 1547.

(18) Numerous structures of MX_4^- salts with $\text{M} = \text{Sb, Bi}$ and $\text{X}^- = \text{halide}$, pseudohalide have been determined by X-ray analysis. Generally, polymeric structures with variable coordination numbers have been found. However, it was shown that in many solids with varying metal-ligand distances MX_4^- moieties with a butterfly structure can be recognized.¹⁹

(19) Sawyer, J. F.; Gillespie, R. J. *Prog. Inorg. Chem.* **1986**, *34*, 65.

(20) Albright, T. A.; Burdett, J. K.; Whangbo, M.-H. *Orbital Interactions in Chemistry*; Wiley: New York, 1985.

(11) Complex ions of s^2 metals may adopt a variety of coordination numbers and geometries. In the solid state the structures can be modified by the counter ion.¹⁰ Nevertheless, at a coordination number of six the complexes are octahedral or nearly so.

(12) Barrowcliffe, T.; Beattie, I. R.; Day, P.; Livingston, K. *J. Chem. Soc. (A)* **1967**, 1810.

(13) Ensinger, U.; Schwarz, W.; Schmidt, A. *Z. Naturforsch.* **1983**, *38B*, 149 and references therein.

(14) Walton, R. A. *Spectrochim. Acta* **1968**, *24A*, 1527.

We suggest that the ground-state distortion of MCl_4^- is eliminated in the excited state. The stabilization of the C_{2v} butterfly structure is essentially lost in the $a'_1 \rightarrow b'_1, a'_1, b'_2$ sp excited state (Figure 3) which rearranges toward a symmetrical tetrahedral geometry. This structural change now explains easily the immense Stokes shift of MCl_4^- .

An analogous approach has been used before in solid-state physics. Blasse and his group have shown that s^2 ions which are doped into host lattices may also show large Stokes shifts if the ions occupy off-center positions in large interstices since these s^2 ions can move toward the center in the sp excited state.³

Acknowledgment. Support of this research by the Deutsche Forschungsgemeinschaft is gratefully acknowledged. We thank Professor G. Blasse for helpful discussions.

Registry No. SbCl_4^- , 18443-80-6; SbCl_6^{3-} , 16283-39-9; BiCl_4^- , 20057-70-9; BiCl_6^{3-} , 15977-99-8.

The Return of the Trapped Electron in X-Irradiated Clathrate Hydrates. An ESR Investigation

Janusz Bednarek,^{§,†} Roland Erickson,[‡] Anders Lund,[‡] and Shulamith Schlick^{*,§}

Department of Chemistry, University of Detroit
Detroit, Michigan 48221

Department of Physics, Linköping University
S-5 81 83 Linköping, Sweden

Received April 24, 1991

The search of an ideal host for the formation and detection of trapped electrons in organic single crystals has led us to a large family of clathrate hydrates containing peralkylammonium hydroxide guests. The presence of trapped electrons has been detected by pulse radiolysis at room temperature in a large number of the clathrates.^{1,2}

Two compounds were chosen for this initial study of electron stabilization: tetramethylammonium hydroxide pentahydrate, $(\text{CH}_3)_4\text{N}^+\text{OH}^- \cdot 5\text{H}_2\text{O}$, mp 335 K (TMNOH, I), and tetra-*n*-butylammonium hydroxide hydrate, $(\text{C}_4\text{H}_9)_4\text{N}^+\text{OH}^- \cdot 31\text{H}_2\text{O}$, mp 303 K (TBNOH, II). This selection was made because the crystal structure for both hydrates has been determined,^{3,4} the melting points are above ambient temperature, and because the amount of water in the stoichiometric compounds is large, about 50% by weight in I and 68% in II; therefore, the radiolytic behavior of these hydrates can be compared to the well-known results for other forms of water (ice, liquid, and glass).

Compound II has the typical crystal structure of most peralkylammonium hydrates based on the pentagonal dodecahedral unit. Compound I is unique among the peralkylammonium hydrates, in that its structure is based on a truncated octahedron and is shown in Figure 1.^{4,5} The distances between the nitrogen (N) in the center and the oxygen atoms of the cage range from 4.30 (to O1) to 4.97 Å (to O2), and the average is 4.61 ± 0.16 Å.

Exciting results have been reported recently on some clathrates, using ^{129}Xe NMR⁶ and gas-phase mass spectroscopic techniques.⁷

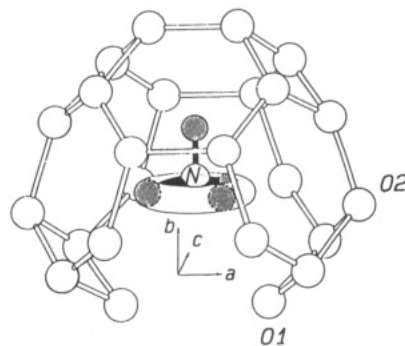


Figure 1. A distorted truncated octahedron containing the $(\text{CH}_3)_4\text{N}^+$ ion in the tetramethylammonium hydroxide clathrate. The three disordered CH_3 groups are represented by the torus and the hydrogen atoms are omitted (redrawn from ref 4).

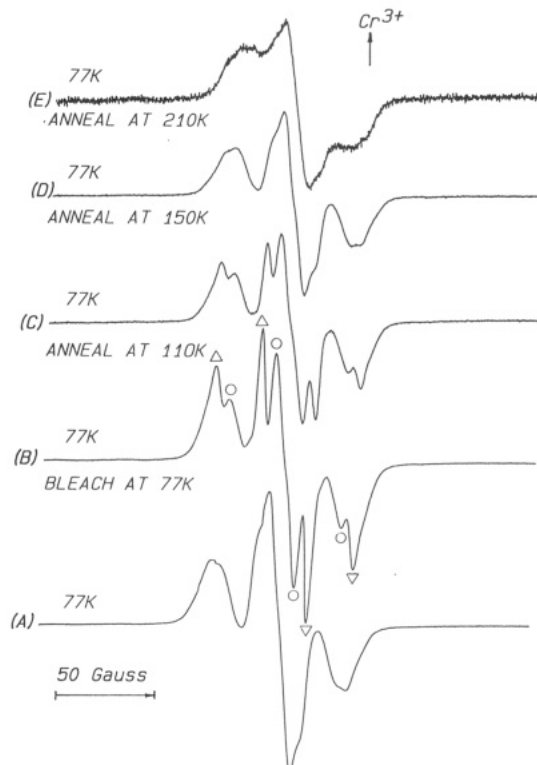


Figure 2. X-band ESR spectra at 77 K of X-irradiated TMNOH clathrate hydrate: (A) immediately after irradiation, (B) after optical bleaching, and (C)–(E), after 3 min annealing at the indicated temperatures. In (B) the signals assigned to the methyl and N-CH_2^{\bullet} radicals are shown by (Δ) and (\circ) , respectively.

The renewed interest in the clathrate hydrates is expected to increase our understanding of this ubiquitous class of compounds.

Crystalline TMNOH and TBNOH were purchased from Fluka. X-irradiations were done for 30–60 min at 77 K in the dark. All ESR measurements were done at 77 K with a Bruker 200D spectrometer operating at 9.7 GHz with 100 kHz modulation, using a low microwave power to prevent saturation of the signal from trapped electrons. Optical bleaching of the irradiated samples was accomplished with a slide projector.

Both TMNOH and TBNOH became intensely blue after X-irradiation in the dark, indicating the presence of trapped electrons. The blue color disappears by optical bleaching.

X-band ESR spectra of irradiated TMNOH clathrate at 77 K are given in Figure 2A–E. Bleaching of the central part of the spectrum is accompanied by resolution enhancement of the remaining signals, as seen in Figure 2B. The spectrum in Figure

* Author to whom correspondence should be addressed.

[†] On leave from the Institute of Applied Radiation Chemistry, Technical University, Lodz, Poland.

[§] University of Detroit.

[‡] Linköping University.

(1) (a) Zagorski, Z. P. *Nucleonika* **1981**, 26, 869. (b) Zagorski, Z. P. *J. Inclusion Phenom. Mol. Recognit. Chem.* **1989**, 7, 569.

(2) (a) Zagorski, Z. P. *Chem. Phys. Lett.* **1985**, 115, 507. (b) Zagorski, Z. P. *J. Phys. Chem.* **1987**, 91, 734. (c) Zagorski, Z. P. *J. Phys. Chem.* **1987**, 91, 972.

(3) McMullan, R.; Jeffrey, G. A. *J. Chem. Phys.* **1959**, 31, 1231.

(4) McMullan, R.; Mak, T. C. W.; Jeffrey, G. A. *J. Chem. Phys.* **1966**, 44, 2338.

(5) Jeffrey, G. A. In *Inclusion Compounds*; Atwood, J. L., Davies, J. E., D., MacNicol, D. D. Eds.; Academic Press: New York, 1984; Vol. 1, p 135.

(6) Ripmeester, J. A.; Ratcliffe, C. I. *J. Phys. Chem.* **1990**, 94, 8773.

(7) (a) Yang, X.; Castleman, A. W., Jr. *J. Am. Chem. Soc.* **1989**, 111, 6845. (b) Yang, X.; Castleman, A. W., Jr. *J. Phys. Chem.* **1990**, 94, 8500. (c) Wei, S.; Shi, Z.; Castleman, A. W., Jr. *J. Chem. Phys.* **1991**, 94, 3268.